

First principles study of pentacene on Au(111)

Kurt Stokbro* and Søren Smidstrup

QuantumWise A/S,

Lersø Parkallé 107,

DK-2100 Copenhagen, Denmark[†]

(Dated: February 27, 2024)

Abstract

We investigate the atomic and electronic structure of a single layer of pentacene on the Au(111) surface using density functional theory. To find the candidate structures we strain match the pentacene crystal geometry with the Au(111) surface, in this way we find pentacene overlayer structures with a low strain. We show that the geometries obtained with this approach has lower energy than previous proposed surface geometries of pentacene on Au(111). We also show that the geometry and workfunction of the obtained structures are in excellent agreement with experimental data.

I. INTRODUCTION

The pentacene crystal(PC) is an important organic electronic material, due to its high hole mobility, and the gold-pentacene interface is one of the most well studied metal-organic interfaces both theoretically¹⁻⁶ and experimentally⁷⁻¹⁷.

It is important to understand the geometry of the pentacene-gold interface, since the interface properties are often close linked to geometric features. However, previous theoretical studies of the interface geometry^{2,3,5} have not shown a systematic approach for determining the lattice parameters of the pentacene overlayer. In this paper we suggest a new approach for determining the pentacene overlayer lattice structure, by strain matching the pentacene crystal with the gold surface. We show that this method will recover the experimentally observed surface geometries and we find that pentacene has a higher adsorption energy in these geometries compared with previously suggested structures.

The paper is organised in the following way: In section II we describe the computational method, and the accuracy of the method is verified for isolated pentacene molecules and the Au(111) surface. In section III we study the structure of a single layer of pentacene on different Au(111) supercells and compare with previous theoretical studies and experimental data. Finally, in section IV we conclude.

II. METHODOLOGY

For the calculations we have used the Atomistix ToolKit (ATK)¹⁸, which is a density-functional theory code using numerical localized atomic basis sets and norm conserving pseudo potentials. For the exchange-correlation potential we have used the Generalized Gradient Approximation (GGA) of Wang and Perdew¹⁹ (PW91) as suggested by Li *et. al*².

The electronic structure is expanded in basis sets optimized to reproduce hydrogen and carbon dimer total energies following the procedure of Blum *et. al*²⁰. For carbon we use 21 orbitals per atom with s, p and d character and ranges up to 3.9 Å, while for hydrogen we use 5 orbitals per atom with s and p character and ranges up to 4.2 Å. The size of the basis set was chosen to converge the ionization energy of a single pentacene molecule as described in section II A. Lee *et. al.* has shown that such long range basis sets can accurately describe the weak gold-pentacene interaction if Basis Set Superposition Errors (BSSE) are accounted

TABLE I. Ionisation energy (E_I) and binding energy per molecule (E_c) for a single pentacene (P1), dimer pentacene (P2), and a pentacene crystal (PC) with lattice parameters from Ref. 21. The experimental ionisation energy of P1 is given in parentheses.

	P1	P2	PC
E_c (eV)	0.0	0.11	0.55
E_I (eV)	6.34 (6.589 ²²)	5.82	5.03

for³. In this study we use the counter poise correction for the BSSE between the gold surface and the pentacene overlayer. In the next section we will show that the computational model gives a good description of the energetics of pentacene molecules.

A. The pentacene molecule and crystal

The first column in Table I shows the calculated ionisation energy of a single pentacene molecule(P1). The ionisation energy was calculated by subtracting total energies of the neutral and charged molecule. Both the neutral and the charged system were relaxed until forces were less than 0.01 eV/Å. The calculations were performed using a computational cell with multipole boundary conditions to properly describe the long range tails of the electro-static potential. The calculated value is 0.25 eV below the experimental value, and we relate this discrepancy to the PW91 exchange-correlation potential.

Next, we study the interaction energy of 2 pentacene molecules (P2). In this case, we correct the total energy and forces for BSSE by using the counterpoise correction for the two pentacene units²³. Accounting for BSSE, we relax the system to 0.01 eV/Å and find an ionisation energy of the dimer having value of 5.82 eV. Therefore, there is reduction of the charging energy by 0.52 eV, since now the positive charge can spread over a pair of molecules.

We calculate the binding energy between the two neutral pentacene molecules to be 0.1 eV/pentacene. Since the PW91 functional does not properly account for Van der Waals interactions the calculated binding energy will be too low. Pratontep *et. al.*²⁴ found the dimer binding energy to be 0.3 eV/pentacene using an Universal Force Field (UFF), in good agreement with experimental data²⁵.

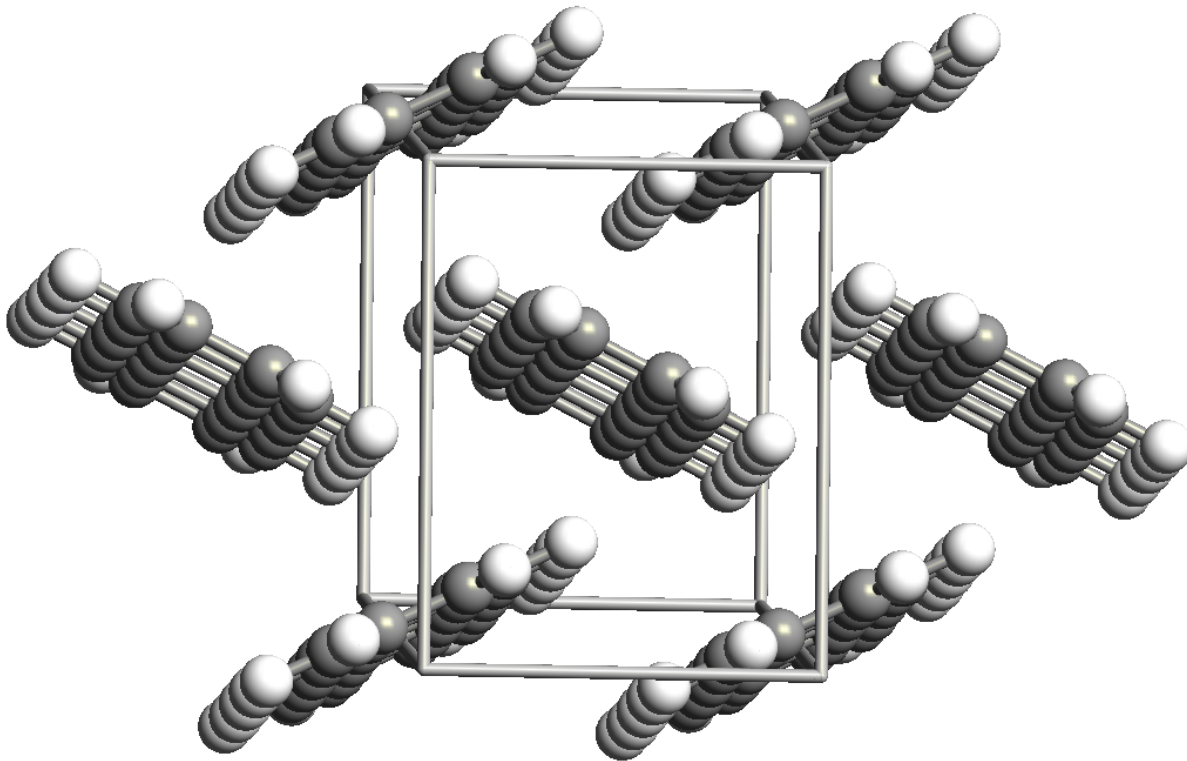


FIG. 1. The figure shows the central pentacene molecule and the 6 surrounding molecules in the relaxed PC. There are 2 pentacene molecules in the unit cell.

Finally we have set up a PC according to the crystallographic data by Sciefer *et. al.*²¹, (P-1: $a=5.985$ Å, $b=7.596$ Å, $c=15.6096$ Å, $\alpha=81.25^\circ$, $\beta=86.56^\circ$, $\gamma=89.8^\circ$). The atomic positions in the unit cell were relaxed using periodic boundary conditions, still applying the BSSE correction to the pentacene units. We found a stress on the unit cell less than 0.003 eV/Å³, and the relaxation of the lattice parameters therefore negligible. The relaxed geometry is illustrated in Fig. 1.

The binding energy per pentacene molecule in the crystal is 0.55 eV, roughly 6 times larger than for the pentacene dimer, in accordance with that the molecules in the PC are surrounded by 6 neighbours. Including Van der Waals interactions will increase this energy substantially.

We also calculated the ionization energy of the PC by performing charged calculations, in this case the charge is neutralized by an uniform background charge. The calculated ionization energy is 5.03 eV, thus a reduction of 1.3 eV compared with the isolated molecule.

B. The Au(111) surface

To simulate gold we use a s,p,d basis set of ranges 2.7-3.6 Å, with a total of 9 orbitals per atom, all other parameters are similar to the pentacene calculations. With this approach we find the lattice constant of gold 4.17 Å in agreement with Li *et. al.*² which also used the PW91 functional (experimental value 4.08 Å).

To test the description of the Au(111) surface we follow Li *et. al.*² and set up a Au(111)-($\sqrt{3}\times 6$) slab consisting of 5 layers with a 15 Å vacuum region above the top layer. Above the top layer we add a layer of gold ghost orbitals to get a better description of the surface. We apply periodic boundary conditions parallel with the surface while we use Dirichlet boundary conditions above the surface and Neumann boundary conditions below the surface. In this way we can properly describe different electrostatic dipoles at the two surfaces. We use a $8\times 3\times 1$ Monkhorst-Pack k-point grid as in Li *et. al.*² and a Fermi-Dirac occupation scheme with room temperature broadening.

The first step is to relax the two upper layers of the gold surface until forces are below 0.01 eV/Å. After relaxation we find a work function of gold of 5.19 eV, slightly below the value of 5.25 eV obtained by Li *et. al.*².

III. PENTACENE ON GOLD

In this section we will investigate the adsorption of pentacene (P1) on the Au(111) surface. Other studies suggest that the interaction between pentacene and the gold surface is weak², thus, the pentacene intermolecular interaction in the adsorption layer must therefore give an important contribution to the adsorption energy. We will assume that this interaction is maximum when pentacene is in its crystal geometry. Our approach to find the geometry of the pentacene adsorption layer is therefore to find a common supercell of the Au(111) surface and the PC. For the PC we will assume that it is adsorbed with the phenyl rings laying flat on the surface, corresponding to an A-C surface plane.

A. Strain matching the surface cells

In the following we discuss our algorithm for finding a common supercell of the Au(111) and PC(010) surfaces. We first generate all possible bravais lattices for the two surfaces,

$$(\vec{v}_1, \vec{v}_2) = N(\vec{a}_1, \vec{a}_2), \quad (1)$$

$$(\vec{u}_1, \vec{u}_2) = M(\vec{b}_1, \vec{b}_2), \quad (2)$$

where \vec{a}_1, \vec{a}_2 are the primitive vectors for the Au(111) surface, N a 2×2 repetition matrix where the entries are integers below a maximum value N_{max} , and \vec{v}_1, \vec{v}_2 the bravais lattice vectors of the supercell. $\vec{b}_1, \vec{b}_2, M, \vec{u}_1, \vec{u}_2$ are the corresponding quantities for the PC(010) surface.

We next determine a rotation matrix, R which rotates \vec{u}_1 over in \vec{v}_1 , and a strain tensor, ε which maps the rotated PC(010) surface lattice onto the Au(111) lattice

$$(\vec{v}_1, \vec{v}_2) = (1 + \varepsilon)R(\vec{u}_1, \vec{u}_2). \quad (3)$$

To match the 2 crystals we generate all surface lattices with $N_{max}, M_{max} < 10$, and for each combination we calculate the strain tensor. Fig. 2 shows the strain of the different combinations as a function of the number of atoms in the unit cell of the combined system. Note that for both the gold and PC we have used the experimental lattice constant. The figure shows that by increasing the number of atoms in the surface cell the strain between the 2 lattices can be reduced.

Table II summarizes the lattices with the lowest strain for a low repetition of the PC(010) surface lattice. The table also include the Au(111)-($\sqrt{3} \times 6$) lattice, as seen from the table the strain is rather large for this structure. The ($\sqrt{3} \times 6$) structure was investigated by Li *et al.*² using the VASP²⁶ code and by comparing with their results we can check the accuracy of our computational approach.

B. Adsorption geometries

In the following we will calculate the relaxed geometry of pentacene on the Au(111)-($\sqrt{3} \times 6$), Au(111)-($2 \times 3\sqrt{3}$), and Au(111)-($2 \times 3\sqrt{7}$) surfaces and compare the adsorption energies. In each case the starting geometry is obtained by matching the PC crystal with the

TABLE II. Strain in the PC(010) lattice to match different Au(111) super cells. The first columns shows the length of the Au(111) surface vectors, the second column the number of pentacene molecules in the cell. ε_{11} , ε_{22} , ε_{12} are the components of the strain tensor applied to the PC surface cell in order to match the gold supercell. $\bar{\varepsilon} = (|\varepsilon_{11}| + |\varepsilon_{22}| + |\varepsilon_{12}|)/3$, is the average strain.

Au(111)	PC(010)	ε_{11}	ε_{22}	ε_{12}	$\bar{\varepsilon}$
$(\sqrt{3} \times 6)$	1	-16.0	10.9	3.3	10.1
$(2 \times 3\sqrt{3})$	1	-3.0	-4.0	2.9	3.3
$(2 \times 3\sqrt{7})$	1	-6.4	-0.54	0.0	2.3
$(2 \times \sqrt{199})$	2	0.2	0.7	3.7	1.5
$(\sqrt{43} \times 7)$	4	-0.8	-0.3	-0.5	0.5
$(\sqrt{103} \times \sqrt{273})$	12	0.0	0.1	0.1	0.1

corresponding Au lattice, setting the initial Au-pentacene distance to 3.1Å. Other details of the relaxation procedure are described in section II.

The geometries of the relaxed configurations are illustrated in Fig. 3. For each relaxed geometry we calculate the pentacene lattice vectors a, b , adsorption height z and adsorption angles θ, ϕ , the definitions of the parameters are illustrated for geometry Au(111)- $(2 \times 3\sqrt{3})$ in Fig. 4. The main results of the geometry optimizations are summarized in Table III together with available experimental data.

We first discuss the comparison of the calculated values for the $(\sqrt{3} \times 6)$ with Li *et. al.*². The latter was done using a plane-wave method, thus, discrepancy with this calculation gives a good estimate of the accuracy of our method. The geometry parameters, a, b, z, θ and ϕ are very similar for the two methods²⁷. In the current work we use a relaxation threshold of 0.01 eV, while Li *et. al.*² use 0.03 eV, this may explain the small discrepancy between the calculations.

The adsorption energy is 0.16 eV higher than the value of Li *et. al.*². This is a rather large deviation, in particular since in the study by Lee *et. al.* they found that a LCAO method with long range orbitals applying the BSSE correction should have an accuracy of 0.02 eV compared with a plane-wave calculation. The adsorption energy is however in good agreement with the work by Lee *et. al.*³ where they found a pentacene-gold interaction energy of -0.28 eV for an isolated pentacene molecule adsorbed on the Au(100) surface³

TABLE III. Data for the relaxed geometries of pentacene on the Au(111) surface, for the $(\sqrt{3} \times 6)$, $(2 \times 3\sqrt{3})$ and $(2 \times 3\sqrt{7})$ supercell. For definition of geometry parameters a , b , z , θ and ϕ , see Fig. 4. E_c is the binding energy of the pentacene on gold. Φ_{Au} is the workfunction of the clean gold surface, Φ is the work function of the surface with the adsorbed pentacene, and $\Delta\Phi$ is the relative change in the surface work function. Reference calculation values for the $(\sqrt{3} \times 6)$ surface from Li *et. al.*^{2,27} are given in the third column.

	$(\sqrt{3} \times 6)$	Li <i>et. al.</i> ²	$(2 \times 3\sqrt{3})$	$(2 \times 3\sqrt{7})$	Exp.
a (Å)	5.11	5.11	5.90	5.90	5.64 ⁹ 5.76 ¹¹ 5.7 ^{12,14}
b (Å)	17.71	17.71	15.44	15.33	14.8 ⁹ 15.0 ¹¹ 15.5 ^{12,14}
z (Å)	3.35	3.1-3.5	3.18	3.17	
θ	40 ⁰	38 ⁰	36 ⁰	34 ⁰	43 ⁰¹⁰ 31 ⁰¹²
ϕ	87 ⁰	81 ⁰	81 ⁰	80 ⁰	
E_c (eV)	-0.29	-0.16	-0.42	-0.42	-1.14 ¹¹
Φ_{Au} (eV)	5.19	5.25	5.19	5.16	5.47 ⁹ 5.4 ¹³ 5.1 ¹⁶
Φ (eV)	4.25	4.29	4.48	4.50	4.52 ⁹ 4.4 ¹³ 4.6 ¹⁶
$\Delta\Phi$ (eV)	-0.94	-0.96	-0.71	-0.66	-0.95 ^{9,11} -1.0 ¹³ -0.5 ¹⁶

using the GGA functional of Perdew-Burke-Ernzerhof²⁸. In the present study there are also interactions within the pentacene molecular layer which should give an additional adsorption energy, in accordance with that our value is slightly higher than the value by Lee *et. al.*. Thus, we are confident in our calculated adsorption energy, and believe that the value reported by Li *et. al.*² is too low.

We also calculated the change in the Au(111) work function upon adsorption of pentacene. We find a reduction by -0.94 eV, in excellent agreement with the -0.96 eV found by Li *et. al.*².

The adsorption geometry and properties of the $(2 \times 3\sqrt{3})$ and $(2 \times 3\sqrt{7})$ structure are almost identical and in the following we will focus on the $(2 \times 3\sqrt{3})$ structure. The adsorption energy in this structure is significantly higher than in the $(\sqrt{3} \times 6)$ structure. It is interesting to divide the adsorption energy into pentacene-pentacene interactions, E^{p-p} , and pentacene-Au(111) interaction, E^{au-p} . This separation of the energy can be obtained by performing a calculation of the pentacene overlayer without the gold surface. For the $(\sqrt{3} \times 6)$ structure

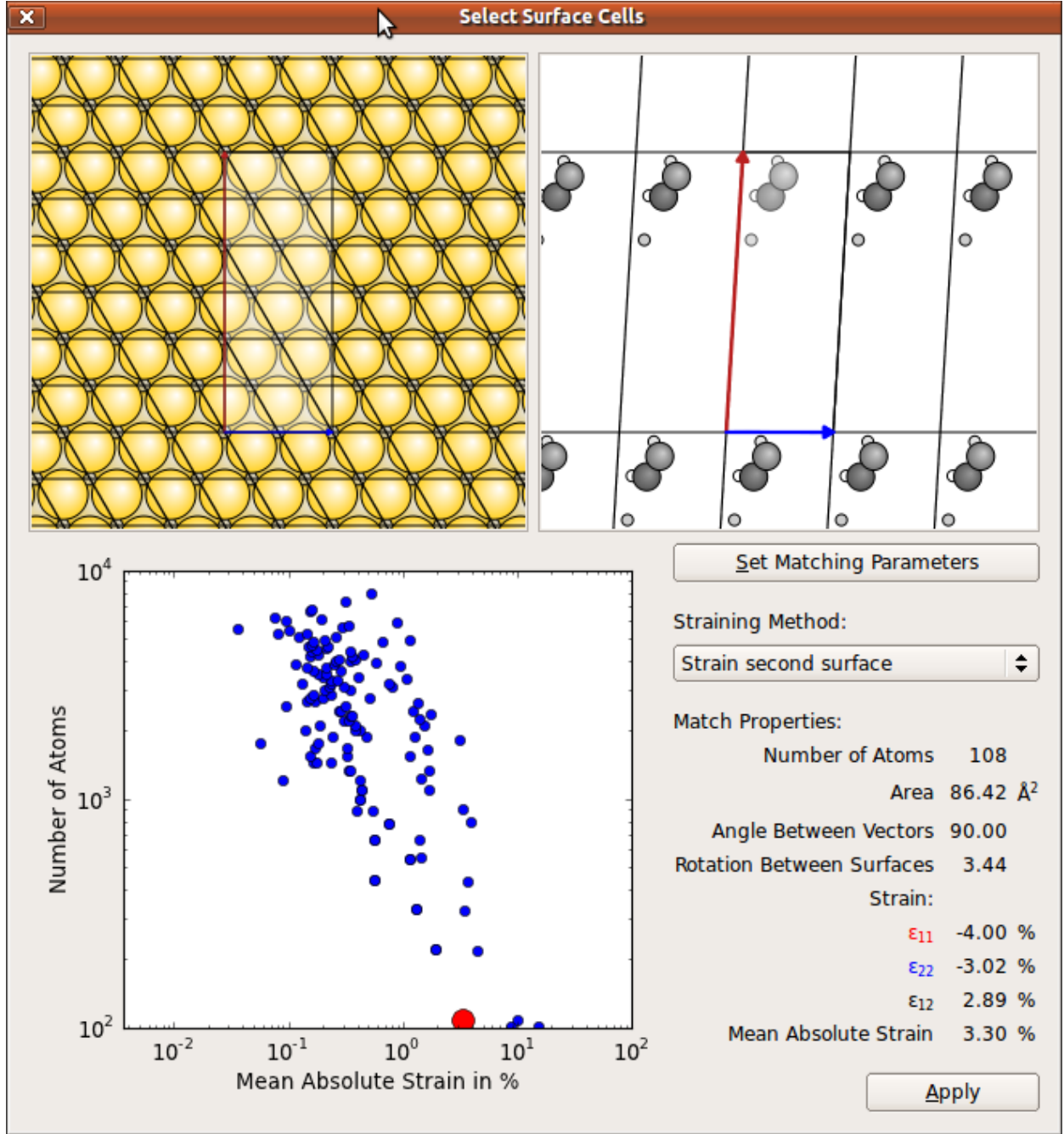


FIG. 2. The graph shows the number of atoms and mean strain for matching a selected sets of Au(111) and PC(010) surface cells. The red dot in the graph corresponds to matching of the Au(111)-(2 \times 3 $\sqrt{3}$) and the PC(010)-(1 \times 1) cell, which has a mean strain of 1.83%.

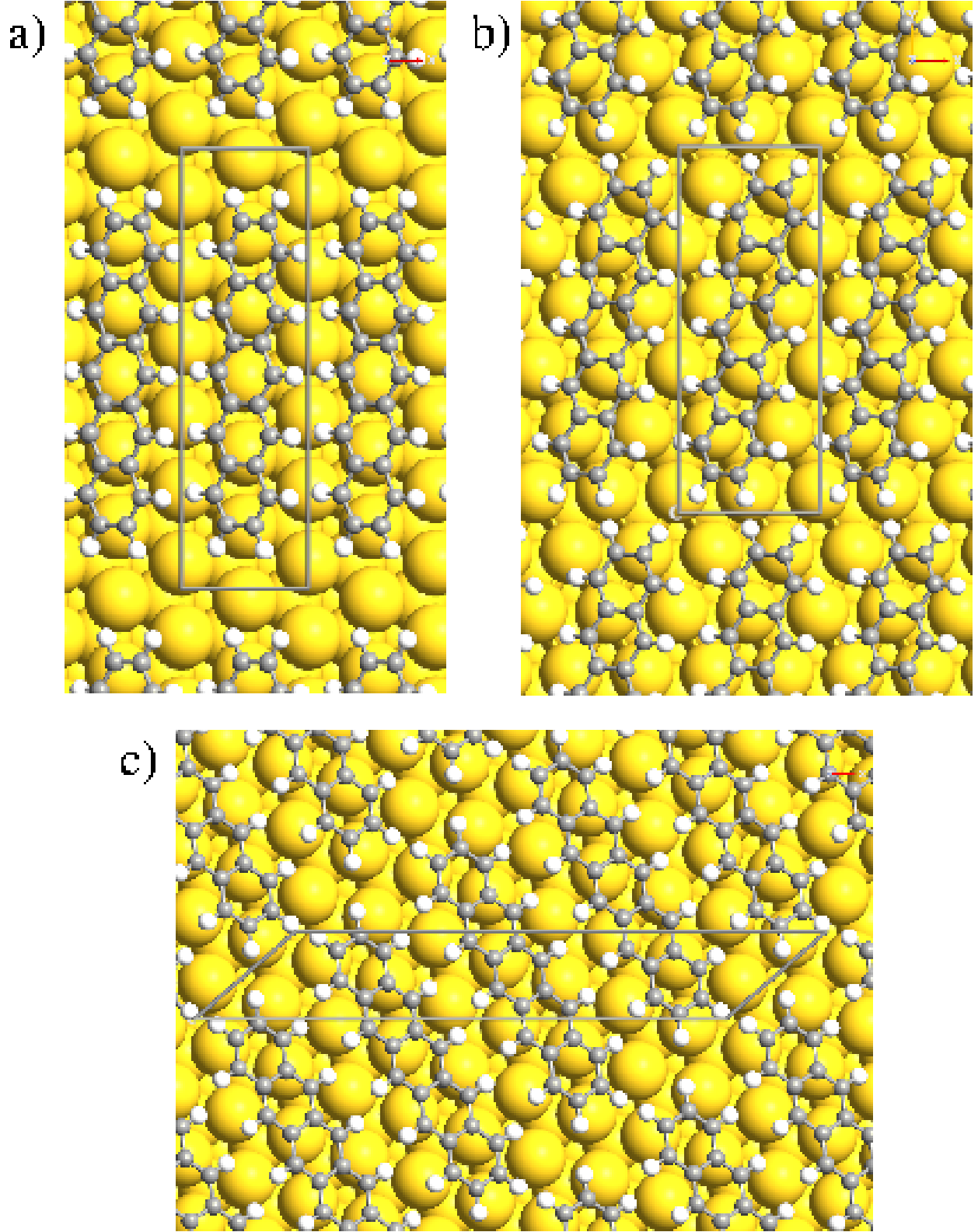


FIG. 3. Top view of the a) $(\sqrt{3} \times 6)$, b) $(2 \times 3\sqrt{3})$, and c) $(2 \times 3\sqrt{7})$ geometry.

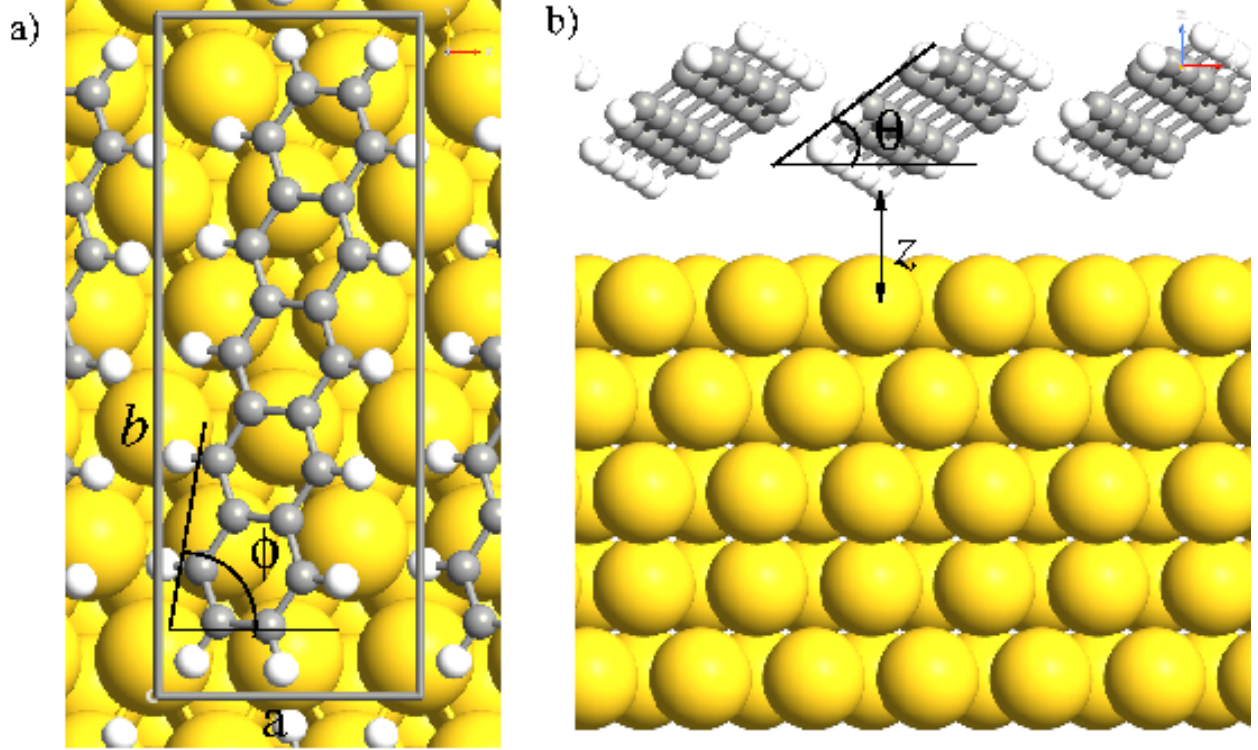


FIG. 4. a) Top view $(2 \times 3\sqrt{3})$ geometry illustrating the pentacene surface lattice parameters a , b and the angle between the pentacene long axis and the a vector, ϕ . b) Side view illustrating the adsorption height, z , and the angle of the molecular plane to the gold surface, θ .

we find $E^{\text{p-p}} = -0.22$ eV and $E^{\text{au-p}} = -0.07$ eV, while for the $(2 \times 3\sqrt{3})$ structure $E^{\text{p-p}} = -0.30$ eV and $E^{\text{au-p}} = -0.12$ eV. Thus, the main difference in the adsorption energy between the two structures arises from a stronger overlayer binding energy in the $(2 \times 3\sqrt{3})$ structure.

The workfunction change upon adsorption of pentacene is -0.71 eV for the $(2 \times 3\sqrt{3})$ geometry, which is significantly lower than what was calculated for the $(\sqrt{3} \times 6)$ surface. Table III shows experimental data for the work function change upon adsorption of pentacene. Note the wide range of values [-1.0 eV, -0.5 eV]. Inspecting the numbers show that the wide spread arises from a spread in the value for the work function of the clean gold surface. The values of the work function for the pentacene covered gold surface seem more reliable and are in the range 4.4-4.6 eV, in excellent agreement with our value for the $(2 \times 3\sqrt{3})$ structure.

Fig. 5 shows the electron density for the combined Au(111)-pentacene system, subtracted the electron density of the separated systems. The result for the $(\sqrt{3} \times 6)$ cell is in excellent

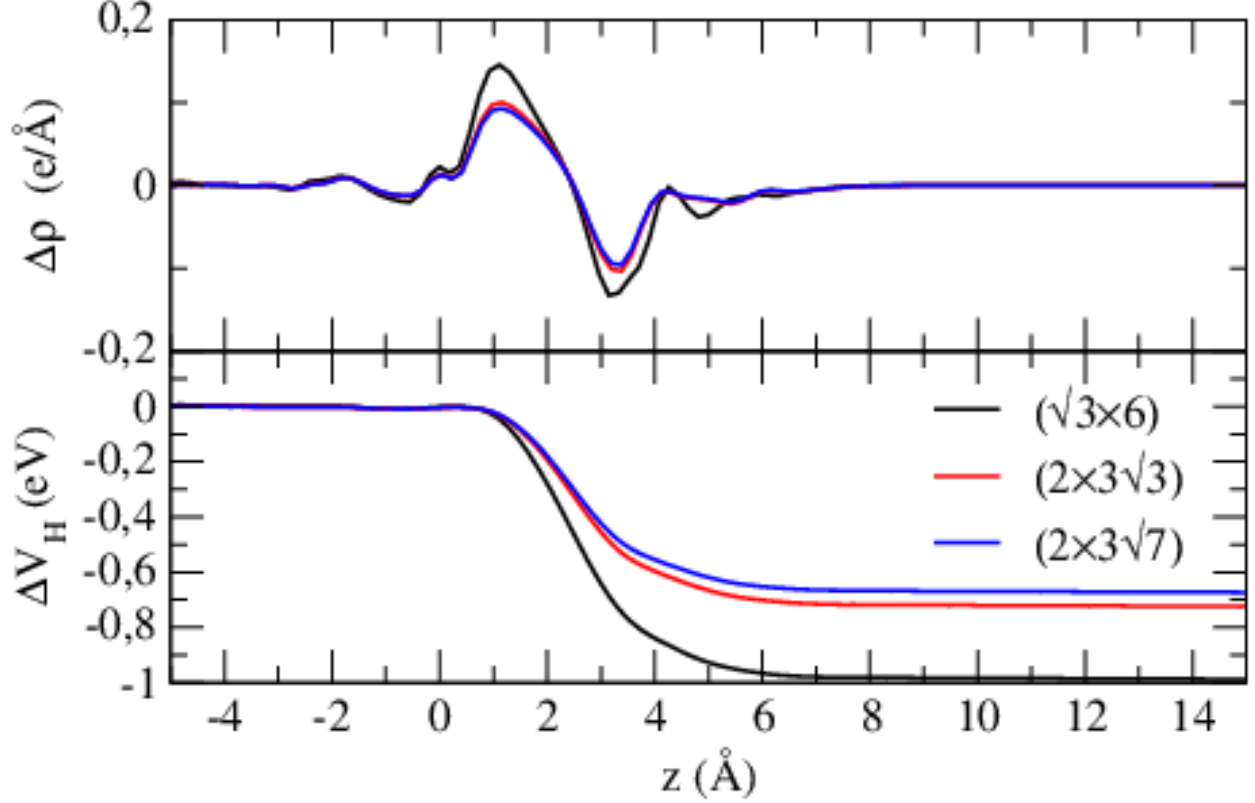


FIG. 5. The induced density and electro-static potential upon adsorption of pentacene on the Au(111) surface for the $(\sqrt{3} \times 6)$ (black), $(2 \times 3\sqrt{3})$ (red), and $(2 \times 3\sqrt{7})$ geometry (blue). $z = 0$ is the position of the top most gold atoms.

agreement with Li *et. al.*². The main change in the density is between the gold surface and the pentacene molecule, and the molecule pushes the density back towards the surface, known as the pillow effect.²⁹ The density change for the $(2 \times 3\sqrt{3})$ surface is qualitatively the same, however, the change in density is slightly smaller and the change in electro-static potential therefore correspondingly lower.

To further investigate the difference between the two systems Fig. 6 shows the Projected Density Of States (PDOS) of the pentacene layer for the 3 systems. We see that the peaks are much broader for the $(\sqrt{3} \times 6)$ system. We relate this to a stronger pentacene-pentacene interaction along the b direction, due to the 15 % smaller lattice constant in this direction compared to the $(2 \times 3\sqrt{3})$ and $(2 \times 3\sqrt{7})$ systems.

We also note that the HOMO is located at the gold fermi level, thus the pentacene crystal will be hole doped by the gold surface. The HOMO-LUMO gap is 1.2 eV, significantly smaller than the 2.2 eV found experimentally for the Au(100) surface⁸, which is related to

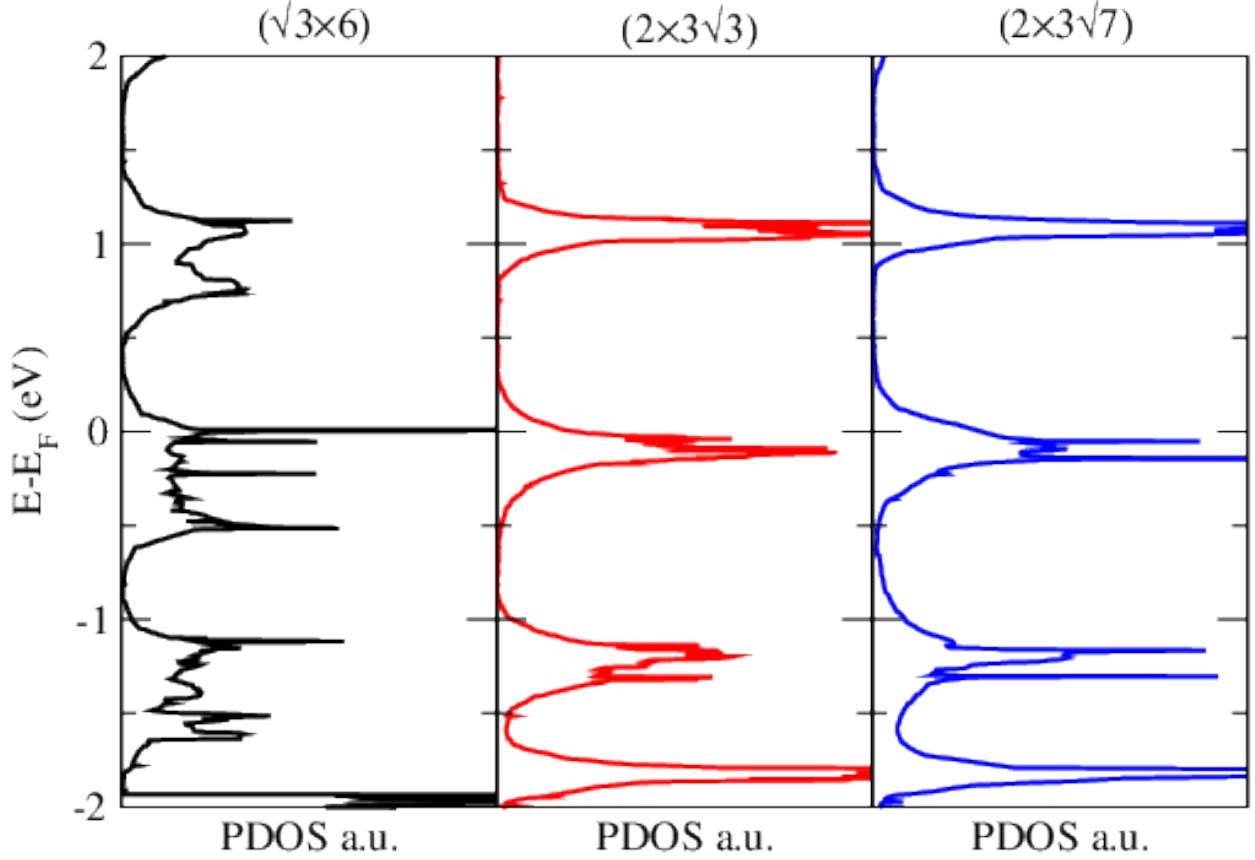


FIG. 6. The Projected Density Of States (PDOS) of the pentacene molecule in the $(\sqrt{3} \times 6)$ (black), $(2 \times 3\sqrt{3})$ (red), and $(2 \times 3\sqrt{7})$ geometry (blue).

the inability of PW91 to accurately describe the unoccupied states, thus, leading to a too small band gap.

IV. CONCLUSIONS

We have investigated the geometry of a single layer of pentacene on the Au(111) surface. We presented a new method for finding the preferred surface lattice of the system by strain matching the pentacene crystal with the Au(111) surface. With this approach we find the $(2 \times 3\sqrt{3})$ structure to have a low strain, and we find that the adsorption energy of this structure is more favourable than the $(\sqrt{3} \times 6)$ structure suggested in a previous study². This structure is in agreement with experimental data for the pentacene surface geometry⁷ and we reproduce the measured workfunction of the pentacene covered Au(111)^{9,13,16}. We suggest that the presented method may be used for determining the adsorption structure of

other weakly adsorbed molecular layers.

ACKNOWLEDGMENTS

We acknowledge Alexander Bratkovski for proof reading the manuscript.

* kurt.stokbro@quantumwise.com

† <http://quantumwise.com>

- ¹ B. Pieczyrak, E. Abad, F. Flores, and J. Ortega, J. Chem. Phys., **135**, 084702 (2011).
- ² H. Li, Y. Duan, V. Coropceanu, and J.-L. Bredas, Organic Electronics, **10**, 1571 (2009).
- ³ K. Lee, J. Yu, and Y. Morikawa, Phys. Rev. B, **75**, 045402 (2007).
- ⁴ K. Lee and J. Yu, Surf. Sci., **589**, 8 (2005).
- ⁵ K. Toyoda, I. Hamada, K. Lee, S. Yanagisawa, and Y. Morikawa, J. Chem. Phys., **132**, 134703 (2010).
- ⁶ G. Saranyaa, S. N. V. Natarajanb, P. Kolandaivela, and K. Senthilkumara, J. Mol. Graph. and Mod., **38**, 334 (2012).
- ⁷ N. Koch, A. Kahn, J. Ghijsen, J. Pireaus, J. Schwartz, R. L. Johnson, and A. Elschner, Appl. Phys. Lett., **82**, 70 (2007).
- ⁸ O. McDonald, A. A. Cafolla, D. Carty, G. Sheerin, and G. Hughes, Surf. Sci., **600**, 3217 (2006).
- ⁹ P. Schroeder, C. B. France, J. B. Park, and B. A. Parkinson, J. Appl. Phys., **91**, 3010 (2002).
- ¹⁰ K. Ihm, B. Kim, T.-H. Kang, K. Kim, M. H. Joo, T. H. Kim, S. S. Yoon, and S. Chung, Appl. Phys. Lett, **89**, 033504 (2006).
- ¹¹ C. B. France, P. Schroeder, J. B. Forsythe, and B. A. Parkinson, Langmuir, **19**, 1274 (2003).
- ¹² D. Käfer, L. Ruppel, and G. Witte, Phys. Rev. B, **75**, 085309 (2007).
- ¹³ N. J. Watkins, L. Yan, and Y. Gao, Appl. Phys. Lett., **80**, 4384 (2002).
- ¹⁴ J. H. Kang and X.-Y. Zhu, Appl. Phys. Lett, **82**, 3248 (2003).
- ¹⁵ W.-H. Soe, C. Manzano, A. D. Sarkar, N. Chandrasekhar, and C. Joachim, Phys. Rev. Lett., **102**, 176102 (2009).
- ¹⁶ L. Diao, C. D. Frisbie, D. D. Schroepfer, and P. P. Ruden, J. Appl. Phys., **101**, 014510 (2007).
- ¹⁷ Z. Liu, M. Kobayashi, B. C. Paul, Z. Bao, and Y. Nishi, Phys. Rev. B, **82**, 035311 (2010).

- ¹⁸ The calculations were performed with Atomistix ToolKit, version ATK-12.8, QuantumWise A/S (2012). <http://quantumwise.com/documents/manuals>.
- ¹⁹ Y. Wang and J. Perdew, Phys. Rev. B, **43**, 8911 (1991).
- ²⁰ V. Blum, R. Gehrke, F. Hanke, P. Havu, X. Ren, K. Reuter, and M. Scheffler, Computer Phys. Comm., **180**, 2175 (2009).
- ²¹ S. Schiefer, M. Huth, A. Dobrinevski, and B. Nickel, J. A. Chem. Soc., **129**, 10316 (2007).
- ²² N. E. Gruhn, D. A. da Silva Filho, T. G. Bill, M. Malagoli, V. Coropceanu, A. Kahn, and J.-L. Bredas, J. Am Chem. Soc., **124**, 7918 (2002).
- ²³ J. Kohanoff, *Electronic Structure Calculations for Solids and Molecules* (Cambridge University Press, 2006).
- ²⁴ S. Pratontep, F. Nüesch, L. Zuppiroli, and M. Brinkmann, Phys. Rev. B, **72**, 085211 (2005).
- ²⁵ Experimental Pentacene Ionization energy is 6.589 eV. <http://astrochemistry.ca.astro.it>.
- ²⁶ G. Kresse and J. Furthmüller, Phys. Rev. B, **54**, 11169 (1996).
- ²⁷ Fig. 2 of Li *et. al.*² shows the total energy as function of distance and the total energy is lowest at $z \sim 3.3$ Å while the authors report $z = 3.13$ Å. To address this discrepancy, the authors put the following comment: “We note that the extreme flatness of the potential energy surface in the range $z \sim 3.1 - 3.5$ Å does not allow for a very accurate determination of the optimal z distance.”.
- ²⁸ J. P. Perdew, K. Burke, and M. Ernzerhof, Phys. Rev. Lett., **77**, 3865 (1996).
- ²⁹ N. Koch, A. Volmer, S. Duhm, Y. Sakamoto, and T. Suzuki, Adv. Mater., **19**, 112 (2007).